NUKLEONIKA 2013;58(3):379–385 ORIGINAL PAPER

EPR spectroscopy of Cu^{2+} and Mn^{2+} in borate glasses

Adam Drzewiecki, Bohdan Padlyak, Volodymyr Adamiv, Yaroslav Burak, Ihor Teslyuk

Abstract. Electron paramagnetic resonance (EPR) spectra of the CaB_4O_7 and $LiCaBO_3$ glasses containing 0.5 and 1.0 mol.% CuO and MnO_2 impurity compounds were investigated at room temperature. The glasses with CaB_4O_7:Cu, $LiCaBO_3$:Cu, CaB_4O_7:Mn and $LiCaBO_3$:Mn compositions were produced from the corresponding polycrystalline compounds using standard glass synthesis and technological conditions developed by the authors. The EPR spectral parameters of the Cu^{2+} and Mn^{2+} centres in both glasses containing 0.5 and 1.0 mol.% CuO and MnO_2 doping oxides were determined. Analysis of EPR spectral parameters shows that Cu impurity is incorporated into the CaB_4O_7 and $LiCaBO_3$ glass network as isolated Cu^{2+} ($3d^9$, $^2D_{5/2}$) paramagnetic ions. The Cu^{2+} ions occupy Ca(Li) sites of the borate glass network coordinated by six O^{2-} anions with geometry of elongated octahedron (D_{4h} symmetry) due to the Jahn--Teller effect. The EPR spectra of the Mn-doped CaB_4O_7 and $LiCaBO_3$ glasses are virtually identical and typical of all oxide glasses activated with Mn^{2+} ($3d^5$, $^6S_{5/2}$) ions. Observed EPR spectra in the Mn-doped glasses were attributed to isolated Mn^{2+} (1) centres ($g_{eff} \cong 4.3$) in octahedral Ca(Li) sites with a strong (fully) rhombic distortion, isolated Mn^{2+} (2) centres ($g_{eff} \cong 2.0$) in octahedral Ca(Li) sites with nearly cubic local symmetry as well as pairs and small clusters of the Mn^{2+} ions, coupled by magnetic dipolar and exchange interactions. On the basis of the obtained results and analysis of referenced data, the local structure of the Cu^{2+} and Mn^{2+} centres in the borate glasses have been proposed.

Key words: borate glasses • Cu^{2+} paramagnetic centre • electron paramagnetic resonance (EPR) spectroscopy • hyperfine structure • Mn^{2+} paramagnetic centre

A. Drzewiecki
Institute of Physics,
University of Zielona Góra,
4a Szafrana Str., 65-516 Zielona Góra, Poland

B. Padlyak✉
Institute of Physics,
University of Zielona Góra,
4a Szafrana Str., 65-516 Zielona Góra, Poland
and Institute of Physical Optics,
23 Dragomanov Str., 79-005 Lviv, Ukraine,
Tel.: +48 68 328 2906, Fax: +48 68 328 2920,
E-mail: B.Padlyak@proton.if.uz.zgora.pl

V. Adamiv, Ya. Burak, I. Teslyuk
Institute of Physical Optics,
23 Dragomanov Str., 79-005 Lviv, Ukraine

Received: 23 October 2012
Accepted: 15 January 2013

Introduction

Borate compounds in glassy (or vitreous) and crystal phases both un-doped and doped with transition and rare-earth elements are interesting from the scientific point of view and a wide range of practical applications including radiation dosimetry, quantum and nonlinear optics and other fields. Due to the technical difficulty of borate single crystals growth, the vitreous borate compounds are more perspective than their crystalline analogies, because practically all borate compounds can be obtained in both crystalline and glassy phases. Typical examples of borate glasses are $Li_2B_4O_7$, $KLiB_4O_7$, CaB_4O_7 and $LiCaBO_3$, which correspond to their well--known crystalline analogies.

The un-doped and doped with Mn, Cu and other impurities borate glasses of different basic compositions are promising materials for neutron dosimeters. Valuable neutron dosimetry features of the borate compounds results from their compositions, because the high content of light atoms such as Li, K, Ca and B makes them tissue-equivalent (effective atomic number of borate compounds is closely similar to the effective atomic number of biological soft tissue), causes low density and high cross-section to capture of high energy neutrons [8]. Low density of the borate materials effects a large neutron to gamma scintillation efficiency ratio which makes them selective neutron scintillation detectors in

the mixed radiation field [18]. On the other hand, borate compounds due to the tissue-equivalent characteristics, high sensitivity and wide range of linear response are promising as personal thermoluminescence dosimeters of relatively high dose of γ- and X-ray radiation [2].

Recent studies of borate compounds mostly concern searching for optimal luminescence activators, in particular Cu and Mn, which are classical photoluminescence activators. Moreover, copper is known as an efficient thermoluminescence activator in the 400÷460 nm spectral range [2], optimal for usage with PPD (pixelated photon detector). One can notice that the modern semiconductor photon detector, consisting of array structure of avalanche photodiodes, is driven by a much lower voltage than the photomultiplier tube.

At present, it is known from optical spectroscopy that the Cu and Mn impurities are incorporated in the structure of the $Li_2B_4O_7$ (lithium tetraborate) crystals and glasses in multivalent states as a Cu^+, Cu^{2+} [5, 13] and Mn^{2+}, Mn^{3+} [6] ions, respectively. The $Li_2B_4O_7$:Cu and $KLiB_4O_7$:Cu tetraborate glasses give two broad emission bands in the 380÷600 nm spectral range with the maxima near 420 and 465 nm, which are related to the $3d^94s \rightarrow 3d^{10}$ metal-centred triplet--singlet transition of the Cu^+ centres with different local environments or their distortion [5, 13]. The Mn-doped borate glasses are characterized by a broad emission band peaked at about 600 nm, belonging to the $^4T_{1g} \rightarrow {}^6A_{1g}$ transition of Mn^{2+} centres in the octahedral sites of glass network [9, 14]. The Cu^{2+} ($3d^9$) and Mn^{3+} ($3d^4$) centres in octahedral sites of the $Li_2B_4O_7$, $KLiB_4O_7$ and $LiCaBO_3$ glasses give a characteristic broad optical absorption band with maxima around 750 nm ($^2B_{1g} \rightarrow {}^2B_{2g}$ transition) [9, 13] and 465 nm ($^5E_g \rightarrow {}^5T_{2g}$ spin-allowed transition) [9, 14], respectively.

It is generally acknowledged that electron and local structure of the paramagnetic and luminescence centres depends on the structure and basic chemical composition of matrix compounds and can be determined by EPR and optical spectroscopy. Original results of EPR spectroscopy of the Cu^{2+} and Mn^{2+} paramagnetic centres in the $Li_2B_4O_7$ and $KLiB_4O_7$ tetraborate crystals and glasses, doped with Cu and Mn were reported in [5, 10, 13, 15]. This paper is devoted to EPR investigation of the electron and local structure of Cu and Mn impurity centres in the CaB_4O_7 and $LiCaBO_3$ glasses containing 0.5 and 1.0 mol.% CuO and MnO_2. Dependencies of EPR spectral parameters of the CaB_4O_7 and $LiCaBO_3$ glasses, doped with Cu and Mn are analyzed in comparison with our previous results, obtained for $Li_2B_4O_7$:Cu, $KLiB_4O_7$:Cu, $Li_2B_4O_7$:Mn and $KLiB_4O_7$:Mn glasses [10, 13, 15]. The optical spectroscopy of the CaB_4O_7 and $LiCaBO_3$ glasses, doped with Cu and Mn will be published in a separate paper.

Experimental details

Synthesis of borate compounds and fabrication of glasses

Composition of the investigated glasses corresponds to the composition of their well-known crystalline analogies. Therefore, the glasses of high optical quality with CaB_4O_7:Cu, $LiCaBO_3$:Cu, CaB_4O_7:Mn and $LiCaBO_3$:Mn compositions were obtained from the corresponding polycrystalline compounds. For solid state synthesis of the CaB_4O_7 and $LiCaBO_3$ polycrystalline compounds, the calcium and lithium carbonates ($CaCO_3$ and Li_2CO_3) and boric acid (H_3BO_3) of high chemical purity (99.999%) were used. The Cu and Mn impurities were added to the raw materials in the form of copper(II) and manganese(IV) oxide compounds (CuO and MnO_2, respectively) in amounts of 0.5 and 1.0 mol.%.

The solid-state synthesis of the CaB_4O_7 and $LiCaBO_3$ polycrystalline compounds was carried out from the raw materials using a multi-step heating process, which can be described by the following chemical reactions:

$$(1)\quad CaCO_3 + H_3BO_3\ (170°C,\ H_2O\uparrow) \rightarrow CaCO_3 + \alpha\text{-}HBO_2\ (250°C,\ H_2O\uparrow) \rightarrow CaCO_3 + B_2O_3\ (800°C,\ CO_2\uparrow) \rightarrow CaB_4O_7$$

$$(2)\quad Li_2CO_3 + H_3BO_3\ (150°C,\ H_2O\uparrow) \rightarrow Li_2CO_3 + \alpha\text{-}HBO_2\ (250°C,\ H_2O\uparrow) \rightarrow Li_2CO_3 + B_2O_3\ (600°C,\ CO_2\uparrow) \rightarrow Li_2B_4O_7 + [Li_2CO_3 + B_2O_3] \rightarrow (800°C,\ CO_2\uparrow) \rightarrow Li_2B_4O_7$$

One can notice that both, (1) and (2), chemical reactions include synthesis of the glass forming boron trioxide (B_2O_3) from boric acid (H_3BO_3) and elimination of the gaseous CO_2 and H_2O.

Large samples of the Cu- and Mn-doped glasses with CaB_4O_7 and $LiCaBO_3$ compositions were obtained by fast cooling of the corresponding melts. The melts were heated up to the temperature at least 100 K higher than their melting temperatures (T_{melt} = 1253 K for CaB_4O_7, T_{melt} = 1050 K for $LiCaBO_3$) in order to exceed glass transition point and then fast cooled to unable the crystallization process. Two types of crucibles, graphite (C) and corundum ceramic (Al_2O_3), were used for obtaining of the investigated glasses. The quality of obtained glasses is practically independent of the type of crucibles. Colour of the Cu-doped glass samples varies depending on the Cu concentration from lightly-blue (CuO content – 0.5 mol.%) to aquamarine (CuO content – 1.0 mol.%). Colour of the Mn-doped glass samples varies depending on the Mn concentration from lightly-brown (MnO_2 content – 0.5 mol.%) to brown (MnO_2 content – 1.0 mol.%). For EPR investigations bulk glass samples were used which give the same EPR spectra as the powdered glass samples.

Experimental equipment

The X-band EPR spectra in the Cu- and Mn-doped $LiCaBO_3$ and CaB_4O_7 glasses were registered at room temperature using a modernized Radiopan SE/X-2013 radiospectrometer, operating in the high frequency (100 kHz) magnetic field modulation mode. The microwave frequency was measured by a Hewlett-Packard 5350B frequency counter. The magnetic field induction was measured by a 20 NMR magnetometer produced by Resonance Technology (Poznań, Poland). Obtained EPR spectra were digitized by an external analog-to-digital converter and stored by means of a PC computer.

Table 1. Spin Hamiltonian parameters of the Cu^{2+} centres in CaB_4O_7:Cu and $LiCaBO_3$:Cu glasses

Glass composition	Amount of CuO (mol.%)	$g_{\|\|}$	$g_{\perp}$	$A_{\|\|}$ (mT)	$A_{\perp}$ (mT)	$\Delta B^{\|\|}_{pp}$ (mT)	$\Delta B^{\perp}_{pp}$ (mT)
CaB_4O_7:Cu	0.5	2.32 ± 0.01	2.06 ± 0.01	15.4 ± 0.5	2.8 ± 0.5	7.1 ± 0.5	1.7 ± 0.5
	1.0	2.32 ± 0.01	2.06 ± 0.01	15.2 ± 0.5	2.8 ± 0.5	6.4 ± 0.5	1.7 ± 0.5
$LiCaBO_3$:Cu	0.5	2.31 ± 0.01	2.06 ± 0.01	14.9 ± 0.5	2.7 ± 0.5	6.4 ± 0.5	1.8 ± 0.5
	1.0	2.31 ± 0.01	2.06 ± 0.01	14.6 ± 0.5	2.7 ± 0.5	6.2 ± 0.5	1.8 ± 0.5

Table 2. The EPR spectral parameters of the Mn^{2+} (2) centres in CaB_4O_7:Mn and $LiCaBO_3$:Mn glasses

Glass composition	Amount of MnO_2 (mol.%)	g_{iso}	A_{iso} (mT)	ΔB_{pp} (mT)
CaB_4O_7:Mn	0.5	2.03 ± 0.01	8.8 ± 0.5	6.2 ± 0.5
	1.0	2.03 ± 0.01	8.8 ± 0.5	6.6 ± 0.5
$LiCaBO_3$:Mn	0.5	2.03 ± 0.01	8.8 ± 0.5	6.4 ± 0.5
	1.0	2.03 ± 0.01	8.9 ± 0.5	6.4 ± 0.5

Table 3. The parameters of EPR signals of the Fe^{3+} centres in the investigated borate glasses

Glass composition	Amount of doping (CuO or MnO_2) compounds (mol.%)	Time constant (s)	g-factor	ΔB_{pp} (mT)
CaB_4O_7:Cu	0.5	3.0	4.31 ± 0.01	4.1 ± 0.5
	1.0	3.0	4.31 ± 0.01	4.2 ± 0.5
$LiCaBO_3$:Cu	0.5	3.0	4.31 ± 0.01	5.1 ± 0.5
	1.0	1.0	4.28 ± 0.01	4.4 ± 0.5
CaB_4O_7:Mn	0.5	3.0	4.31 ± 0.01	5.1 ± 0.5
	1.0	3.0	4.30 ± 0.01	5.8 ± 0.5
$LiCaBO_3$:Mn	0.5	1.0	4.28 ± 0.01	5.0 ± 0.5
	1.0	1.0	4.28 ± 0.01	6.0 ± 0.5

The spin Hamiltonian and EPR spectral parameters gathered in Tables 1–3 were calculated using the positions of resonance lines (B_r) in the experimental EPR spectra and work microwave frequency of the radiospectrometer. The resonance field and peak-to--peak derivative linewidth (ΔB_{pp}) for each component of the EPR spectrum were taken as arithmetic mean of the measured B_r and ΔB_{pp} values. For paramagnetic centres Cu^{2+} and Mn^{2+} contained hyperfine component multiplet structures (Tables 1 and 2) and the resonance field was calculated as arithmetic mean of the measured B_r values for two middle lines of multiplet and g-factor was calculated using the obtained, by such a way, resonance field and measured microwave frequency. The hyperfine constant (A) was calculated as arithmetic mean of difference of the resonance field values of neighbouring lines, and ΔB_{pp} is arithmetic mean of this parameter for each line in multiplet.

Recorded EPR spectra of the shape, typical of the glass samples and the used equipment features allow to estimate uncertainty of the microwave frequency and magnetic field induction measurements to ± 10 kHz and ± 0.25 mT, respectively. Uncertainties of the calculated spin Hamiltonian and EPR spectral parametrs were estimated according to the total differential method. The uncertainty of the A and ΔB_{pp} parameters uncertainty is taken as the double uncertainty of magnetic field measurement due to the method of their calculation. The g-factor uncertainties depend on g-values range. In particular, for $g \cong 2$ and $g \cong 4.3$ the calculated uncertainties equals ± 0.002 and ± 0.007, respectively. However, concerning the type and quality of the analyzed EPR spectra, especially lack of some parts of multiplet structures, we decided to enlarge uncertainty of the measured g-factor in both ranges to ± 0.01.

Results and discussion

EPR spectra of the Cu-doped glasses with CaB_4O_7 and $LiCaBO_3$ compositions

The EPR spectra of the CaB_4O_7:Cu and $LiCaBO_3$:Cu glasses containing different amount of CuO are presented in Figs. 1 and 2. As one can see from Fig. 1, the EPR spectra for both glassy matrices and both concentrations of Cu dopant are closely similar and consist of two intensive four component bands, centred at $g \cong 2.3$ and $g \cong 2.06$, which belong to the Cu^{2+} ($3d^9$, $^2D_{5/2}$) paramagnetic ions. The latter quadruplet was also registered in the narrow magnetic field range and is presented separately in Fig. 2. Sharp line at $g \cong 4.3$ belongs to the Fe^{3+} paramagnetic centres, which are discussed in section 'EPR signals of the Fe^{3+} non-controlled impurity in the CaB_4O_7 and $LiCaBO_3$ glasses'. Observed EPR spectra of the Cu^{2+} centres are typical of disordered,

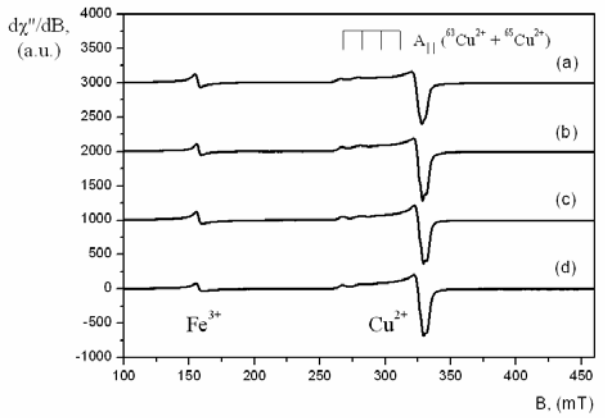

Fig. 1. EPR spectra of the CaB_4O_7:Cu (a, b) and $LiCaBO_3$:Cu (c, d) glasses containing 0.5 mol.% (a, c) and 1.0 mol.% (b, d) CuO.

particularly glassy compounds including borate glasses [10, 13, 15]. Observed EPR line quadruplets (Figs. 1 and 2) are related to the hyperfine structure caused by the interaction of unpaired electron spin ($S = 1/2$) with nuclei of the ^{63}Cu and ^{65}Cu isotopes (natural abundance – 69.1% and 30.9%, respectively, nuclear spin $I = 3/2$ for both isotopes). One can notice that the hyperfine components belonging to nuclei of the ^{63}Cu and ^{65}Cu isotopes are not resolved in the observed EPR spectra (Figs. 1 and 2), because their nuclear magnetic moments are closely similar (nuclear magnetic moment is 7.1% higher for ^{65}Cu than that for ^{63}Cu).

Observed EPR spectra of the Cu^{2+} centres in the investigated borate glasses can be satisfactorily described by spin Hamiltonian of axial symmetry in the following form:

$$\hat{H} = g_{||}\mu_B B_z \hat{S}_z + g_{\perp}\mu_B (B_x \hat{S}_x + B_y \hat{S}_y) + A_{||}\hat{S}_z \hat{I}_z + A_{\perp}(\hat{S}_x \hat{I}_x + \hat{S}_y \hat{I}_y) \quad (3)$$

where μ_B is the Bohr magneton, $g_{||}$ and $g_{\perp}$ are principal values of the axial g-tensor, $A_{||}$ and $A_{\perp}$ are principal values of the axial A-tensor describing hyperfine structure. The spin Hamiltonian parameters of the Cu^{2+} centres in CaB_4O_7:Cu and $LiCaBO_3$:Cu glasses, calculated from their experimental EPR spectra recorded at room temperature are presented in Table 1. As can be seen in Table 1, the $g_{||}$ and $g_{\perp}$ values are practically independent of the CuO dopant concentration and basic glass matrix composition within the uncertainty of measurement range. The g-factor values for Cu^{2+} centres in the CaB_4O_7:Cu and $LiCaBO_3$:Cu glasses are also consistent with our previous results for $Li_2B_4O_7$:Cu and $KLiB_4O_7$:Cu glasses. For all investigated glasses with $Li_2B_4O_7$:Cu, $KLiB_4O_7$:Cu, CaB_4O_7:Cu and $LiCaBO_3$:Cu compositions the Cu^{2+} g-values equals $g_{||} = (2.31 \div 2.32) \pm 0.01$ and $g_{\perp} = 2.06 \pm 0.01$ [10, 13, 15]. Obtained g-factor values and powder type shaped spectrum are characteristic of all oxide glasses doped with Cu^{2+} [16]. Such EPR spectra are characteristic of Cu^{2+} ($3d^9$) ions coordinated by six O^{2-} ligand anions arranged in the octahedron, elongated along the principal axis (tetragonally distorted octahedron of D_{4h} symmetry group) due to Jahn-Teller effect. On the basis of the relation $g_{||} > g_{\perp} > g_e = 2.0023$ for the obtained g-factor values, one can conclude that the ground state of unpaired electron of the Cu^{2+} centres in borate glasses is $^2B_{1g}$ ($d_{x^2-y^2}$ orbital). For all investigated borate glasses, the hyperfine constants of the Cu^{2+} centres are equal to $= (14.6 \div 15.5) \pm 0.5$ mT and $A_{\perp} = (2.7 \div 2.9) \pm 0.5$ mT [10, 13, 15]. Some small differences of the hyperfine constants for Cu^{2+} centres can be related to different cationic environment in their second coordination shell that leads to the different interatomic distances in the first coordination shell (oxygen coordinated octahedron). According to [17], the local environments of cations in the structure of oxide glasses and corresponding crystals are similar. Thus, the location of Cu^{2+} impurity centres in the Ca (Li) cationic sites of the investigated borate glasses with sixfold coordination to oxygen as in the corresponding borate crystals can be expected.

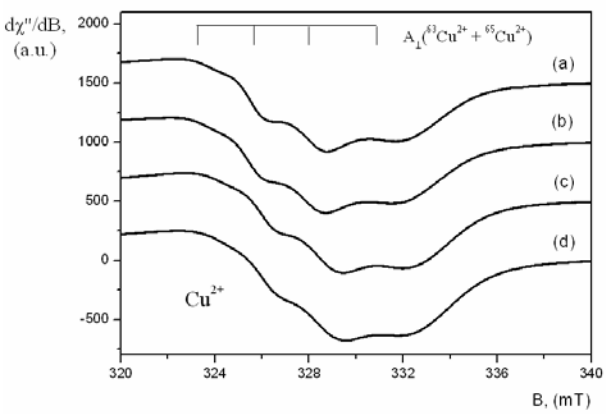

Fig. 2. The central part of EPR spectra of the CaB_4O_7:Cu (a, b) and $LiCaBO_3$:Cu (c, d) glasses containing 0.5 mol.% (a, c) and 1.0 mol.% (b, d) CuO.

EPR spectra of the Mn-doped glasses with CaB_4O_7 and $LiCaBO_3$ compositions

The EPR spectra of the CaB_4O_7:Mn and $LiCaBO_3$:Mn glasses containing different amount of MnO_2, registered at room temperature are presented in Figs. 3 and 4. The observed spectra for both glassy matrices and both Mn dopant concentrations are closely similar and consist of broad band signal centred near $g_{eff} \cong 4.3$ signed as Mn^{2+} (1) and intensive broad (peak-to-peak derivative linewidth, $\Delta B_{pp} \cong 50$ mT) band centred near $g_{eff} \cong 2.0$ containing six almost equidistant well-resolved hyperfine components, signed as Mn^{2+} (2). One can notice that a sharp EPR signal with $g_{eff} \cong 4.3$ coming from Fe^{3+} paramagnetic centres discussed later in section 'EPR signals of the Fe^{3+} non--controlled impurity in the CaB_4O_7 and $LiCaBO_3$ glasses' is observed (Fig. 3). The broad unresolved EPR band centred at $g_{eff} \cong 2.0$ was also registered in the narrow magnetic field range for all investigated Mn-doped glasses (Fig. 4). Six well-resolved components of the Mn^{2+} (2) signal are related to hyperfine structure, caused by nuclei of the ^{55}Mn isotopes (natural abundance – 100%, nuclear spin $I = 5/2$). The Mn^{2+} (1) and Mn^{2+} (2) EPR signals belong to the isolated (non-interacting) Mn^{2+} ($3d^5$, $^6S_{5/2}$) ions. A broad unresolved response centred at $g_{eff} \cong 2.0$ according to [4, 14] can be attributed to the Mn^{2+} pair centres, coupled by magnetic dipolar interaction and to small exchange-coupled Mn^{2+} clusters.

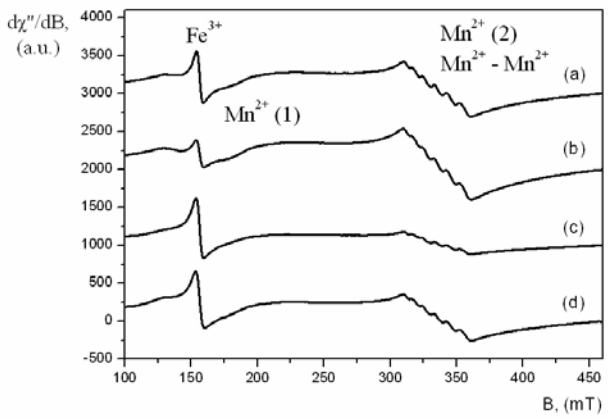

Fig. 3. EPR spectra of the CaB_4O_7:Mn (a, b) and $LiCaBO_3$:Mn (c, d) glasses containing 0.5 mol.% (a, c) and 1.0 mol.% (b, d) MnO_2.

One can notice that optical spectroscopy besides the Mn^{2+} ($3d^5$) centres also shows presence of the Mn^{3+} ($3d^4$) centres, which reveals in the optical absorption spectra [9]. Although, for doping of the investigated glasses was used the MnO_2 compound containing Mn(IV), characteristic EPR and optical spectra of the Mn^{4+} ($3d^3$) paramagnetic centres were not observed in the CaB_4O_7:Mn and $LiCaBO_3$:Mn glasses. This result correlates with the published results of optical and EPR spectroscopy of the $Li_2B_4O_7$:Mn and $KLiB_4O_7$:Mn glasses [6, 10, 15]. Absence of the Mn^{4+} ions in the investigated borate glasses can be explained by the difficulties of charge compensation at $Mn^{4+} \rightarrow Li^+$ (Ca^{2+}) heterovalence substitution.

The observed EPR spectra of the Mn^{2+} ions are characteristic of glasses and other disordered compounds [4, 14]. The EPR spectrum of the isolated Mn^{2+} centres in the investigated borate glasses can be described by spin Hamiltonian in the following form

$$\hat{H} = \mu_B (B \cdot g \cdot \hat{\mathbf{S}}) + D[\hat{S}_z^2 - 1/3S(S+1)] + E(\hat{S}_x^2 - \hat{S}_y^2) + \hat{\mathbf{I}} \cdot A \cdot \hat{\mathbf{S}} \quad (4)$$

where μ_B is the Bohr magneton, g is the factor of spectroscopic splitting, D and E are the axial and orthorhombic zero-field splitting (ZFS) terms, respectively. At present time, it is generally acknowledged [1, 4] that the Mn^{2+} (1) signal with $g_{eff} \cong 4.3$ originates from isolated $3d^5$ ions

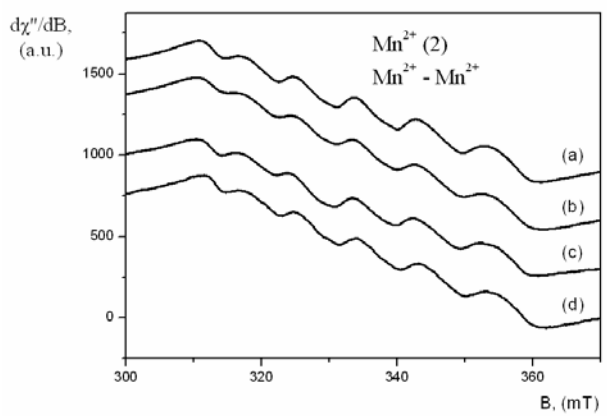

Fig. 4. The central part of EPR spectra of the CaB_4O_7:Mn (a, b) and $LiCaBO_3$:Mn (c, d) glasses containing 0.5 mol.% (a, c) and 1.0 mol.% (b, d) MnO_2.

(Fe^{3+} and Mn^{2+}) for a large second-order ligand ZFS in which the value of $|E/D|$ ratio lies in the vicinity of its maximum value of 1/3 ($|E/D| = 1/3$) that corresponds to fully rhombic distortion. Several types of fully rhombic distortions of the sixfold (octahedral) and fourfold (tetrahedral) oxygen-coordinated sites were considered in [1]. According to [1, 4, 11], the Mn^{2+} (1) EPR signal with $g_{eff} \cong 4.3$, observed in the Mn-doped CaB_4O_7 and $LiCaBO_3$ glasses belong to isolated Mn^{2+} centres in the octahedrally-coordinated sites with a strong (fully) rhombic distortion. Taking into account the interpretation of the Mn^{2+} EPR spectra in oxide glasses given in [4, 11, 14], we can conclude that the isolated Mn^{2+} centres occupy octahedral sites of the CaB_4O_7 and $LiCaBO_3$ glass network with strong (fully) rhombic distortion (Mn^{2+} (1) centres with $g_{eff} \cong 4.3$) and the sites with nearly cubic local symmetry (Mn^{2+} (2) centres with $g_{eff} \cong 2.0$).

The EPR spectral parameters of the Mn^{2+} (2) centres, collected in Table 2, were calculated from experimental EPR spectra of the CaB_4O_7:Mn and $LiCaBO_3$:Mn glasses containing 0.5 and 1.0 mol.% MnO_2. As can be seen in Table 2, the g-factor (g_{iso}) and hyperfine constants (A_{iso}) values are the same within the uncertainty of measurement range and thus are independent of the basic glass composition and Mn dopant concentration. Obtained values of the Mn^{2+} (2) spectral parameters are consistent with our previous studies of the Mn-doped borate glasses with $Li_2B_4O_7$ and $KLiB_4O_7$ compositions [10, 15]. In particular, for Mn^{2+} (2) centres in all investigated Mn-doped borate glasses the g-factor values is equal to 2.03 ± 0.01 and their hyperfine structure constants lie in the (8.7÷8.9) ± 0.1 mT range [10, 15]. The ΔB_{pp} values for Mn^{2+} (2) centres in the CaB_4O_7:Mn glasses slightly increases with increasing Mn dopant concentration due to homogeneous broadening of the EPR lines, whereas for Mn^{2+} (2) centres in the $LiCaBO_3$:Mn glasses this phenomenon was not observed (Table 2). The g-factor (g_{iso}) and hyperfine constant (A_{iso}) values for Mn^{2+} (2) centres are practically independent (in the framework of experimental errors) of the basic glass composition and Mn concentration (Table 2).

Based on the obtained EPR results and structural data for CaB_4O_7 and $LiCaBO_3$ glasses [12], one can conclude that the Mn^{2+} impurity ions are incorporated in Ca(Li) sites of the CaB_4O_7 and $LiCaBO_3$ glass network with coordination number to oxygen $N = 6 \div 7$, because according to [17], the local environments in the oxide glasses are closely similar to the corresponding crystals with the same chemical composition. So, the isolated Mn^{2+} centres occupy octahedral Ca(Li) sites with strong (full) rhombic distortion (Mn^{2+} (1) centres) and octahedral Ca(Li) sites with nearly cubic symmetry (Mn^{2+} (2) centres) of the CaB_4O_7 and $LiCaBO_3$ glasses. The lowering of coordination number from 7 to 6 can be related to the presence of oxygen vacancies in the glass network.

EPR signals of the Fe^{3+} non-controlled impurity in the CaB_4O_7 and $LiCaBO_3$ glasses

The EPR spectra of all investigated CaB_4O_7 and $LiCaBO_3$ glasses, doped with Cu and Mn contain a

sharp EPR signal centred at $g_{eff} \cong 4.3$ (Figs. 1 and 3). The same EPR signal was also observed in the previously investigated $Li_2B_4O_7$ and $KLiB_4O_7$ glasses, doped with Cu and Mn [10, 13, 15]. At present time, it is generally acknowledged [1, 4, 11] that this isotropic EPR signal with $g_{eff} \cong 4.3$ is attributed to the Fe^{3+} ($3d^5$, $^6S_{5/2}$) non--controlled impurity ions, which can be described by spin Hamiltonian (4) without hyperfine structure term. One can notice that the presence of Fe^{3+} signal with $g_{eff} = (4.28 \div 4.31) \pm 0.01$ indicates the classical glass structure of the investigated samples [1, 3, 11, 15].

In Table 3 are presented spectral parameters of the Fe^{3+} EPR signals (g-factor and ΔB_{pp} values) in the investigated glasses. As can be seen, for the given glass matrix (CaB_4O_7 or $LiCaBO_3$) and doping compounds (CuO or MnO_2) the g-factor values are independent of dopant concentration within uncertainty of measurements range. The linewidth of the Fe^{3+} EPR signals increases with increasing Cu and Mn dopant concentrations as long as the spectra recorded with the same time constant value can be compared (recording time constant affects measured linewidth and middlepoint of recorded asymmetric EPR line due to its distortion by signal lowpass filtering in the EPR spectrometer) (Table 3). So, one can state that the iron (Fe^{3+}) impurity is incorporated to the glass matrix as non-controlled ingredient with the transitional metal oxides dopants. This result is consistent with our previous EPR investigations of other borate glasses, doped with Cu and Mn [10, 13, 15].

Conclusions

According to our results presented in this work and previous investigations [10, 13, 15] of EPR spectra of the $Li_2B_4O_7$, $KLiB_4O_7$, CaB_4O_7 and $LiCaBO_3$ glasses, doped with Cu and Mn in different concentration we can conclude that the copper and manganese impurities are incorporated into the all investigated borate glasses network as paramagnetic Cu^{2+} ($3d^9$, $^2D_{5/2}$) and Mn^{2+} ($3d^5$, $^6S_{5/2}$) ions. The Mn^{2+} ions are incorporated into the investigated borate glasses network as isolated centres and small exchange-coupled clusters for a low and high Mn concentration, whereas the Cu^{2+} ions are incorporated into the borate glass structure as isolated centres for both, a low and high Cu concentration.

The Cu^{2+} EPR spectra in the borate glasses are typical of disordered, particularly glassy, compounds and are characterized by the axially-symmetric g-factor and hyperfine constant values. The spin Hamiltonian parameters of the Cu^{2+} centres for $Li_2B_4O_7$:Cu, $KLiB_4O_7$:Cu, CaB_4O_7:Cu and $LiCaBO_3$:Cu glasses containing different amount of the CuO, determined at room temperature are almost independent of the basic glass composition and Cu impurity concentration. Some differences in hyperfine constants for Cu^{2+} centres in the investigated borate glasses are related to slight differences in their local environments (interatomic distances). According to the obtained spin Hamiltonian parameters one can conclude that the Cu^{2+} centres in the borate glasses are coordinated by six O^{2-} anions with geometry of octahedron, elongated along the principal axis (tetragonally distorted octahedron, D_{4h} symmetry group) due to the Jahn-Teller effect. The ground state of the Cu^{2+} impurity centres in the investigated borate glasses is $^2B_{1g}$ ($d_{x^2-y^2}$ orbital).

The Mn^{2+} centres in all the investigated borate glasses are characterized by the EPR spectra, which are typical of other glassy compounds. The observed EPR spectra in all the investigated Mn-doped borate glasses were attributed to isolated Mn^{2+} centres, located in octahedral sites with strong (fully) rhombic distortion (Mn^{2+} (1) centers with $g_{eff} \cong 4.3$) and the sites with nearly cubic local symmetry (Mn^{2+} (2) centers with $g_{eff} \cong 2.0$) as well as to pairs and small clusters of the Mn^{2+} ions in the borate glass network. The EPR spectral parameters of isolated Mn^{2+} (2) centres (g_{iso} and A_{iso}) for $Li_2B_4O_7$:Mn, $KLiB_4O_7$:Mn, CaB_4O_7:Mn and $LiCaBO_3$:Mn glasses containing different amount of MnO_2, determined at room temperature, practically are independent of the basic glass composition and Mn impurity concentration.

The increasing of dopant (Cu and Mn) concentration leads to homogeneous broadening of EPR lines of the Fe^{3+} impurity centres. Increasing of linewidth of the Fe^{3+} signal with increasing MnO_2 and CuO amounts allows to conclude that the doping compounds are the main source of the iron (Fe^{3+}) non-controlled impurity in the investigated borate glasses.

Acknowledgment. This work was supported by the Ministry of Education, Science, Youth and Sport of Ukraine (project No. 0111U001627) and the University of Zielona Góra (Poland).

References

1. Brodbeck CM, Bukrey RR (1981) Model calculations for the coordination of Fe^{3+} and Mn^{2+} ions in oxide glasses. Phys Rev B 24:2334–2342
2. Can N, Karali T, Townsend PD, Yildiz F (2006) TL and EPR studies of Cu, Ag and P doped $Li_2B_4O_7$ phosphor. J Phys D: Appl Phys 39:2038–2043
3. Castner T Jr, Newell GS, Holton C, Slichter CP (1960) Note on the paramagnetic resonance of iron in glass. J Chem Phys 32:668–673
4. Griscom DL (1980) Electron spin resonance in glasses. J Non-Cryst Solids 40:211–272
5. Ignatovych M, Holovey V, Vidoczy T *et al.* (2005) Spectroscopy of Cu- and Ag-doped single crystal and glassy lithium tetraborate: luminescence, optical absorption and ESR study. Funct Mater 12:313–317
6. Ignatovych M, Holovey V, Vidoczy T, Baranyai P (2007) Spectral study on manganese- and silver-doped lithium tetraborate phosphors. Radiat Phys Chem 76:1527–1530
7. Ignatovych M, Holovey V, Watterich A *et al.* (2004) Luminescence characteristics of Cu- and Eu-doped $Li_2B_4O_7$. Radiat Meas 38:567–570
8. Ishii M, Kuwano Y, Asaba S *et al.* (2004) Luminescence of doped lithium tetraborate single crystals and glass. Radiat Meas 38:571–574
9. Padlyak BV, Drzewiecki A, Adamiv VT, Burak YaV, Teslyuk IM (2011) Synthesis and spectroscopy of the $LiCaBO_3$ glasses, doped with manganese and copper, functional and nanostructured. Joint Conferences on Advanced Materials, 6–9 September 2011, Szczecin. In: Materials FNMA'11, 1:77–78
10. Padlyak BV, Drzewiecki A, Smyrnov OO (2010) EPR

spectroscopy of tetraborate glasses, doped with Mn and Cu. Curr Top Biophys 33;Suppl A:171–175
11. Padlyak BV, Gutsze A (1998) EPR study of the impurity paramagnetic centres in (CaO-Ga_2O_3-GeO_2) glasses. Appl Magn Reson 14:59–68
12. Padlyak BV, Mudry SI, Kulyk YO *et al*. (2012) Synthesis and X-ray structural investigation of undoped borate glasses. Materials Science-Poland 30:264–273
13. Padlyak B, Ryba-Romanowski W, Lisiecki R *et al*. (2010) Synthesis and spectroscopy of tetraborate glasses doped with copper. J Non-Cryst Solids 356:2033–2037
14. Padlyak B, Vlokh O, Kukliński B, Sagoo K (2006) Spectroscopy of Mn-doped glasses of CaO-Ga_2O_3-GeO_2 system. Ukr J Phys Opt 7:1–10
15. Padlyak BV, Wojtowicz W, Adamiv VT, Burak YaV, Teslyuk IM (2010) EPR spectroscopy of the Mn^{2+} and Cu^{2+} centres in lithium and potassium-lithium tetraborate glasses. Acta Phys Pol A 117:122–125
16. Pilbrow JR (1990) Transition ion electron paramagnetic resonance. Clarendon Press, Oxford
17. Witkowska A, Padlyak B, Rybicki J (2008) An EXAFS study of the local structure of rare-earth luminescence centres in the $3CaO$-Ga_2O_3-$3GeO_2$ glass. Opt Mater 30:699–702
18. Zadneprovski BI, Eremin NV, Paskhalov AA (2005) New inorganic scintillators on the basis of LBO glass for neutron registration. Funct Mater 12:261–268